ORIGINAL ARTICLE

Neonatal Pulmonary Magnetic Resonance Imaging of Bronchopulmonary Dysplasia Predicts Short-Term Clinical Outcomes

Nara S. Higano[1], David R. Spielberg[1], Robert J. Fleck[2], Andrew H. Schapiro[2], Laura L. Walkup[1], Andrew D. Hahn[3], Jean A. Tkach[2], Paul S. Kingma[4], Stephanie L. Merhar[4], Sean B. Fain[3,5], and Jason C. Woods[1,2]

[1]Center for Pulmonary Imaging Research, Division of Pulmonary Medicine and Department of Radiology, [2]Department of Radiology, and [4]Division of Neonatology and Pulmonary Biology, Cincinnati Children's Hospital, Cincinnati, Ohio; and [3]Department of Medical Physics and [5]Department of Radiology, University of Wisconsin–Madison, Madison, Wisconsin

ORCID ID: 0000-0002-6233-161X (N.S.H.).

Abstract

Rationale: Bronchopulmonary dysplasia (BPD) is a serious neonatal pulmonary condition associated with premature birth, but the underlying parenchymal disease and trajectory are poorly characterized. The current National Institute of Child Health and Human Development (NICHD)/NHLBI definition of BPD severity is based on degree of prematurity and extent of oxygen requirement. However, no clear link exists between initial diagnosis and clinical outcomes.

Objectives: We hypothesized that magnetic resonance imaging (MRI) of structural parenchymal abnormalities will correlate with NICHD-defined BPD disease severity and predict short-term respiratory outcomes.

Methods: A total of 42 neonates (20 severe BPD, 6 moderate, 7 mild, 9 non-BPD control subjects; 40 ± 3-wk postmenstrual age) underwent quiet-breathing structural pulmonary MRI (ultrashort echo time and gradient echo) in a neonatal ICU–sited, neonatal-sized 1.5 T scanner, without sedation or respiratory support unless already clinically prescribed. Disease severity was scored independently by two radiologists. Mean scores were compared with clinical severity and short-term respiratory outcomes. Outcomes were predicted using univariate and multivariable models, including clinical data and scores.

Measurements and Main Results: MRI scores significantly correlated with severities and predicted respiratory support at neonatal ICU discharge ($P < 0.0001$). In multivariable models, MRI scores were by far the strongest predictor of respiratory support duration over clinical data, including birth weight and gestational age. Notably, NICHD severity level was not predictive of discharge support.

Conclusions: Quiet-breathing neonatal pulmonary MRI can independently assess structural abnormalities of BPD, describe disease severity, and predict short-term outcomes more accurately than any individual standard clinical measure. Importantly, this nonionizing technique can be implemented to phenotype disease, and has potential to serially assess efficacy of individualized therapies.

Keywords: bronchopulmonary dysplasia; magnetic resonance imaging; prematurity; neonatal lung disease; outcome prediction modeling

Bronchopulmonary dysplasia (BPD) is a serious neonatal pulmonary condition often associated with premature birth, but the underlying parenchymal disease and clinical trajectory are poorly characterized (1–4). Although infants affected by this condition account for a small percentage of live births (10,000–15,000 new cases reported each year) (1, 5, 6), they represent a high percentage of neonatal healthcare costs (7) and are present in over 60% of our neonatal ICU (NICU) patients at

(Received in original form November 20, 2017; accepted in final form May 23, 2018)

Supported by the Perinatal Institute at Cincinnati Children's Hospital, the Hartwell Foundation at University of Wisconsin–Madison, and NIH grants P01 HL070831, T32 HL007752, T32 CA009206, and K12 HL119986-04.

Author Contributions: Study design—N.S.H., D.R.S., L.L.W., and J.C.W.; data collection—N.S.H., D.R.S., R.J.F., A.H.S., A.D.H., J.A.T., P.S.K., S.L.M., and S.B.F.; analysis—N.S.H., D.R.S., and J.C.W.; manuscript drafting, editing, and approval—all authors.

Correspondence and requests for reprints should be addressed to Jason C. Woods, Ph.D., Cincinnati Children's Hospital, 3333 Burnet Avenue, ML 5033, Cincinnati, OH 45229. E-mail: jason.woods@cchmc.org.

Am J Respir Crit Care Med Vol 198, Iss 10, pp 1302–1311, Nov 15, 2018

Originally Published in Press as DOI: 10.1164/rccm.201711-2287OC on May 23, 2018
Internet address: www.atsjournals.org

At a Glance Commentary

Scientific Knowledge on the Subject: Bronchopulmonary dysplasia (BPD) is a common and serious pulmonary complication of premature birth and is defined by treatment with supplemental oxygen for at least 28 days. Its severity is graded by clinically assessed need for respiratory support, which can vary with institutional standards. The underlying parenchymal disease, structural pathology, and disease trajectory are not well characterized. Patients with BPD have higher risks of respiratory complications at later ages, but there exist few strong prognostic indicators of later outcomes.

What This Study Adds to the Field: Radiological evaluation of tomographic, pulmonary magnetic resonance imaging (MRI) in early life can describe disease severity and predict short-term respiratory outcomes in neonatal patients with BPD better than individual standard clinical measures, without requiring sedation or ionizing radiation. These results support the wider implementation of pulmonary MRI in early life as a clinical measure and predictor of lung disease trajectories. Importantly, visualization of regional and structural pathologies via MRI may help in the near future to phenotype disease and to serially monitor efficacy of personalized BPD therapies.

Cincinnati Children's Hospital. As clinical respiratory care and survival rates of extremely preterm infants continue to improve, we will likely see an increased prevalence of patients suffering respiratory sequelae related to prematurity.

The current National Institute of Child Health and Human Development (NICHD)/NHLBI consensus definition of BPD is based only on use of oxygen for at least 28 days (not necessarily consecutive) and a clinically assessed need for supplemental respiratory support at a fixed postmenstrual age (PMA) depending on gestational age (GA) at birth (6), which can vary with institutional standards. However, debate continues on the utility of this and other definitions of BPD, with concerns that diagnosis at a single time point does not adequately predict a neonatal patient's risk for lung disease in later childhood (8–12). Indeed, there are currently few prognostic indicators of later outcomes, with inadequate clinical ability to reliably predict the levels and durations of respiratory support. Furthermore, clinical outcomes in infants with developmental pulmonary insufficiency are often impacted by critical comorbidities, such as pulmonary hypertension (PH), with difficulty in discerning the relative contributions of vascular and parenchymal lung abnormalities to a patient's hypoxemic condition (13, 14).

The current standard of care for BPD infants includes chest X-ray radiograph for management guidance, whereas X-ray computed tomography (CT) scans may be used in more severe cases to further discern underlying pathology. However, there are concerns regarding the ionizing radiation exposure associated with CT, particularly for the nontrivial cumulative exposures from longitudinal monitoring in pediatric and neonatal populations (15–17). Furthermore, even with low-dose CT protocols, neonatal CTs often require sedation and intubation for those patients not already intubated, exposing patients to additional medical risks (18, 19). As such, CT is not a preferred method for serial diagnostic imaging of neonatal BPD.

As a nonionizing modality, magnetic resonance imaging (MRI) is particularly appropriate for the repeated radiological assessment of pulmonary pathologies associated with BPD (20). Indeed, quantitative MRI has seen some initial successes using conventional Cartesian sequences, such as a gradient echo (GRE), to distinguish parenchymal intensities between neonates with and without BPD using intensity thresholding (21). Because a typical GRE sequence implements an echo time (TE) on order with the parenchymal effective transverse relaxation time (T_2^*; ~2 ms at 1.5 T) (22), such acquisitions tend to perform adequately in the low flip-angle (FA) regime in visualizing the volumetric density of high-density tissues (such as fibrosis or inflammation), which have long T_2^* values relative to TE. However, GRE acquisitions suffer to some degree in visualizing the volumetric density of normal or hypodense lung tissues (alveolar simplification, emphysema, cysts, etc.), which have short T_2^* values relative to TE. This work can be refined using ultrashort echo time (UTE) radial/spiral acquisition sequences (23–25). Historically, pulmonary MRI has faced challenges related to the low proton density of the lung parenchyma (26), the aforementioned short parenchymal T_2^*, and image artifacts from cardiac, respiratory, and bulk motion, all of which are significant considerations in a rapidly breathing, noncompliant neonate. UTE MRI implements TE values (typically less than a few hundred microseconds) much shorter than the parenchymal T_2^* to combat the rapid proton signal decay, and has the added value of relative robustness to motion artifacts (24). Because of this relatively short TE value, UTE MRI is ideal for visualizing volumetric densities of hyperdense, normal, or hypodense lung tissue. Furthermore, UTE MRI has recently been shown to accurately quantify neonatal parenchymal density by direct comparison to CT (27), and, as shown previously, sedation is not necessary to obtain high-quality neonatal pulmonary MR images using both GRE and UTE sequences (21, 24–27).

In this work, we performed both GRE and UTE ^{1}H MRI for comprehensive pulmonary structural images of diagnostic quality that could be used in future clinical studies. We hypothesized that pulmonary neonatal MRI can predict short-term respiratory outcomes for infants diagnosed with BPD and can provide image-based phenotyping of disease severity. Because pulmonary MRI can be used safely for serial assessment, this technique has the potential to define the underlying structural abnormalities and trajectory of neonatal pulmonary disease associated with extremely preterm birth. Some of the results of this work have been previously reported in the form of abstracts (28–30).

Methods

Study Subjects

Subjects were recruited from the NICU with Institutional Review Board approval and informed parental consent. Inclusion

criteria for patients with BPD included: history of prematurity (<37-wk GA); clinically diagnosed BPD according to the current NICHD/NHLBI consensus definition; and 48 weeks or less PMA at MRI. Inclusion criteria for control patients included: full-term birth (≥37-wk GA) or preterm birth without BPD; no clinically suspected or apparent lung disease; and 48 weeks or less PMA at MRI. Exclusion criteria for patients with BPD included: evidence of congenital issues that may affect lung development; suspected muscular dystrophy or neurologic disorder that may affect lung development; significant genetic or chromosomal abnormalities that may affect lung development; evidence of any respiratory infection at the time of imaging; and standard MRI exclusion criteria. Exclusion criteria for control patients were the same as for patients with BPD, with the addition of evidence of congenital diseases that may affect lung development (such as congenital heart disease, congenital diaphragmatic hernia, or other systemic pulmonary disease).

The study cohort was comprised of 42 neonates with varying levels of BPD severity, enrolled in a distribution reflective of our inpatient population: 20 with severe BPD; 6 with moderate BPD; 7 with mild BPD; 4 preterm control subjects who were born at less than 37-weeks GA, but were not diagnosed with BPD; and 5 term control subjects who were born at 37-weeks or greater GA, and were primarily diagnosed with seizures or gastrointestinal issues. Further demographic information for the cohort is given in Table 1.

Patients were fed, swaddled, and equipped with ear protection before imaging. Contrast agent was not administered as part of the imaging protocol, and subjects were free breathing and nonsedated, unless respiratory support or sedation was part of their ongoing NICU care. Approximately 30% and 35% of the cohort were sedated and on positive-pressure ventilation (PPV), respectively, for clinical reasons independent of the research MRI exam; no patient was administered sedation or underwent a change in respiratory support for the purposes of imaging. All subjects' heart rates and oxygen saturation (as measured by pulse oximetry) levels were monitored by NICU staff throughout each exam.

Table 1. Subject Group Demographics

BPD Severity (NICHD/NHLBI)	Cohort Size (*n*)	Sex (*M/F*)	GA (*wk*)	PMA at MRI (*wk*)	Birth Weight (*g*)
Term control	5	3/2	39 ± 1	42 ± 1	3,270 ± 520
Preterm control	4	1/3	35 ± 1	39 ± 2	2,510 ± 390
Mild BPD	7	6/1	27 ± 1	37 ± 2	1,160 ± 230
Moderate BPD	6	5/1	27 ± 2	38 ± 2	990 ± 260
Severe BPD	20	10/10	25 ± 2	41 ± 3	690 ± 170

Definition of abbreviations: BPD = bronchopulmonary dysplasia; GA = gestational age; MRI = magnetic resonance imaging; NICHD = National Institute of Child Health and Human Development; PMA = postmenstrual age.
Data are presented as *n* or mean ± SE.

MRI

Neonatal research MRI exams were performed on a unique, small-footprint, neonatal 1.5 T MRI system (originally marketed as an orthopedic scanner from ONI Medical Systems; currently GE Healthcare) sited within our institution's NICU (31–34). The scanner has a 21.8-cm bore size (reduced to 18 cm with the insertion of a quadrature body coil), accommodating neonates up to approximately 4.5 kg, and operates with GE HDx software.

Two ^{1}H MRI sequences were used for pulmonary structural imaging and scoring: a conventional three-dimensional (3D) GRE sequence and a research 3D radial UTE sequence (23–25, 27). For some patients, only GRE ($n = 5$) or only UTE images ($n = 1$) were acquired, due to subject agitation or sustained bulk motion. Typical axial GRE acquisition parameters were: TE = 1.9 ms; repetition time (TR) = 7 ms; FA = 4°; bandwidth = ±90.9 kHz; field of view = 18 cm; pixel resolution = 0.70–0.86 mm; slice thickness = 3 mm; number of averages = 5–10; and scan time = ∼5 min. Typical UTE acquisition parameters were: TE = 0.2 ms; TR = 5 ms; FA = 5°; bandwidth = ±125 kHz; field of view = 18 cm; 3D isotropic resolution = 0.70–0.86 mm (in-plane isotropic pixel resolution identical to slice thickness); scan time = ∼10–16 minutes; and number of radial projections = ∼120,000–200,000. Parameters for UTE acquisitions were chosen to yield a highly proton-density-weighted intensity regime. UTE images were reconstructed after discarding data acquired during bulk motion intervals, via a previously published technique that uses the self-navigating property of non-Cartesian (radial, or UTE) k-space trajectories (25).

MRI Scoring of Lung Disease

Imaging-based lung disease severity was independently assessed by two radiologists blinded to patients' diagnoses (R.J.F., with 22 yr of experience, and A.H.S., with 6 yr of experience) using a modified Ochiai scoring system (21) that includes seven categories (Table 2), with varying visualization quality from GRE and UTE image contrast weighting for each category, as indicated. Each category was scored 0–2, with a total range of 0–14. All image sets were anonymized, with UTE and GRE image sets for a single subject evaluated together to yield one MRI score per radiologist for each subject. A final mean MRI score was generated for each subject by averaging the two radiologists' total scores.

Statistical Analysis

Interreader reliability of MRI scoring was evaluated using a single-rater–type intraclass correlation coefficient test for absolute agreement.

Univariate ANOVA tests (ANOVA; SAS 9.3, SAS Institute Inc.) were used to determine group differences in MRI scores, birth weight, and GA for three outcomes: *1*) BPD severity levels as defined by NICHD diagnostic criteria (mild, moderate, severe, or deceased from lung disease); *2*) levels of respiratory support at NICU discharge (room air, oxygen, ventilator, or death); and *3*) levels of respiratory support at 40-weeks PMA (room air, noninvasive oxygen [either nasal cannula or high-flow nasal cannula], or ventilator). We had intended *a priori* to include a group of patients on noninvasive positive pressure (i.e., continuous positive airway pressure, but no subjects used this interface by 40-weeks PMA.

Multivariable linear regression models were used to analyze three continuous

Table 2. Radiological Scoring System for Pulmonary Magnetic Resonance Imaging of Neonatal Bronchopulmonary Dysplasia, with Respective Image Contrast Weighting Contributions from Ultrashort Echo Time and Gradient Echo Magnetic Resonance Imaging Sequences

Category	Scoring			Quality of Visualization with Sequence Image Contrast Weighting	
	0	1	2	UTE	GRE
Hyperexpansion	None	Focal	Global	Strong	Strong
Mosaic lung attenuation	None	Unclear	Obvious	Strong	Moderate
Emphysema, number of cysts/regions	None	Single	Multiple	Strong (TE $<$ parenchymal T_2*)	Poor (TE $\approx$ parenchymal T_2*)
Emphysema, size	None	$<$5 mm	$>$5 mm	Strong (TE $<$ parenchymal T_2*)	Poor (TE $\approx$ parenchymal T_2*)
Fibrous/interstitial, triangular subpleural opacities	None	1–3 lobes	4–6 lobes	Moderate	Strong
Distortion of bronchovascular bundles	Mild	Moderate	Severe	Moderate	Strong
Subjective impression	Mild	Moderate	Severe	Strong	Strong

Definition of abbreviations: GRE = gradient echo; T_2* = effective transverse relaxation time; TE = echo time; UTE = ultrashort echo time
With its very short TE ($\sim$0.2 ms), UTE images visualize short-T_2* tissue better than GRE images (TE, $\sim$2 ms). For similar reasons, the GRE can yield improved contrast between thicker or more consolidated lung and normal/hypodense parenchyma

outcomes: *1*) duration of ventilator support; *2*) duration of any PPV (ventilator or noninvasive pressure); and *3*) duration of any support (ventilator, noninvasive pressure, or oxygen). Duration was censored to 150 days of life in all cases, a time frame that captured the support at hospital discharge, but avoided excess leverage from patients on respiratory support for years. Models were built for three continuous predictor variables: MRI score; GA; and birth weight. A stepwise selection process was implemented, such that predictors that satisfied *P* less than 0.2 were entered into the model, but were removed if they did not then satisfy *P* less than 0.05.

A general linear model (SAS 9.3) was used to assess the significance of additional

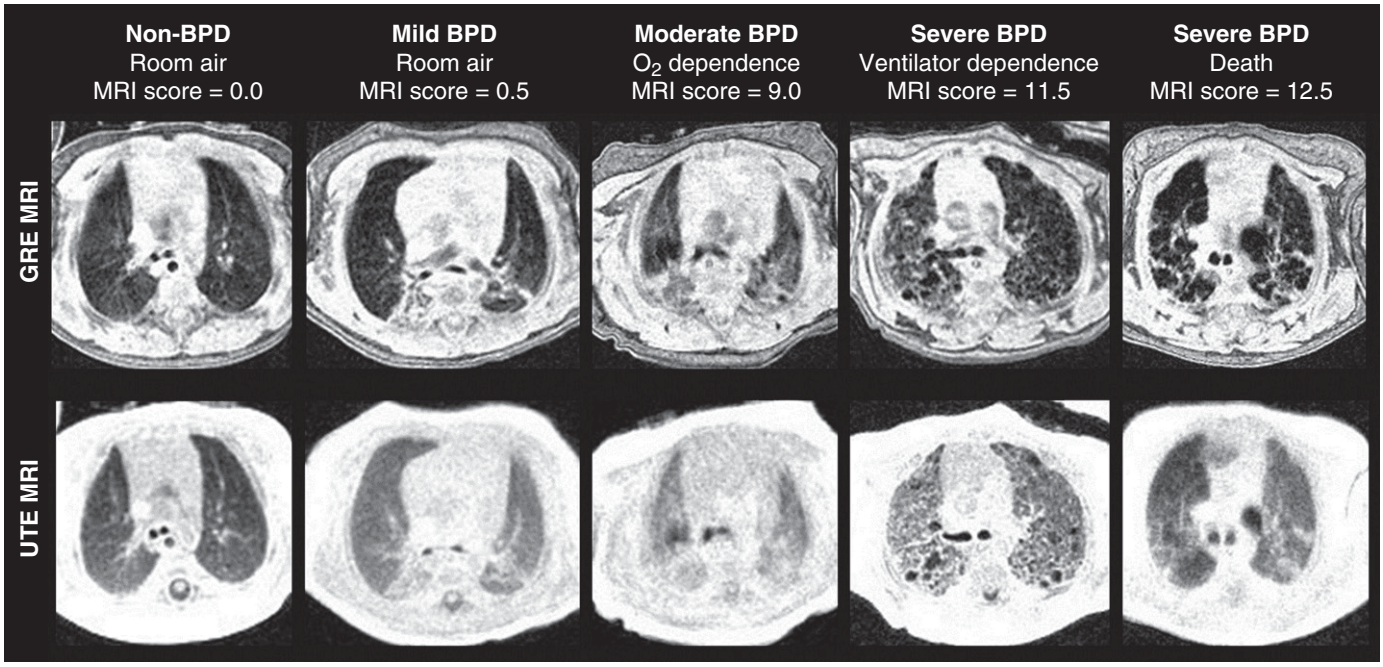

Figure 1. Representative axial gradient echo (GRE) and ultrashort echo time (UTE) magnetic resonance imaging (MRI) demonstrating the range of bronchopulmonary dysplasia (BPD) severity. The level of respiratory support at neonatal ICU discharge and MRI scores are provided for each subject. Owing to its relatively short TE value, the UTE sequence can visualize hypodense tissue with intensity above the noise floor, whereas, in the same tissue, the GRE image is reconstructed with intensity near that of noise, even when non-zero density is present and apparent on UTE (for example, in the deceased severe BPD case at far right). In this way, UTE contrast weighting yields density-like intensities between various pulmonary tissues. On the other hand, with its relatively long TE value, the GRE sequence can yield improved contrast between fibrotic/interstitial/soft tissues and normal/hypodense parenchymal tissues, even though it does not represent accurate density measures of tissue with rapid effective transverse relaxation time decay.

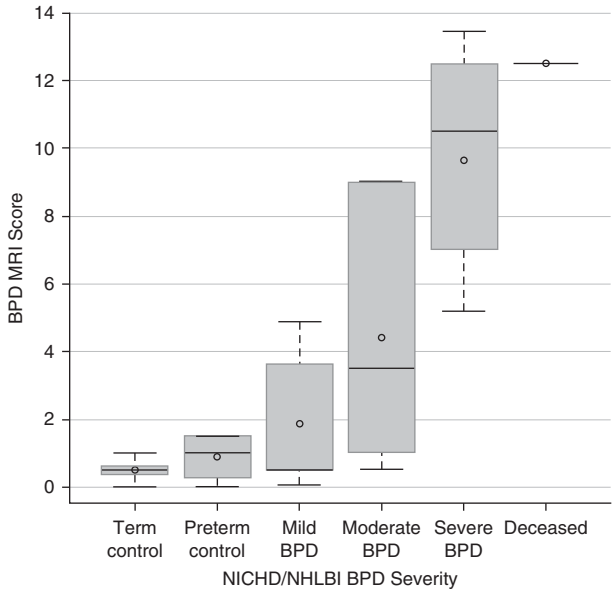

Figure 2. Correlation between magnetic resonance imaging (MRI) score and bronchopulmonary dysplasia (BPD) disease severity (National Institute of Child Health and Human Development [NICHD]/NHLBI definition). Notably, MRI scores of preterm subjects without BPD and term control subjects did not significantly differ, and there is a large standard deviation in MRI scores of patients with moderate and severe BPD, reflective of the broad range of outcomes observed in these severity groups. Plot elements are represented as follows: mean (circle); median (horizontal line); interquartile range (gray box); and 9–91% data (whiskers).

continuous and categorical variables. Preliminary models included all recorded clinical data that may impact support duration, with both continuous variables (MRI score, GA, and birth weight) and categorical variables (sex, race, intrauterine growth restriction [IUGR], multiparity of the pregnancy, postnatal growth failure, patent ductus arteriosus, atrial septal defect, diuretics at MRI, antenatal steroids, postnatal steroids, surfactant, highest level of respiratory support in NICU, systemic PH medications, whether patients had a pneumonia while in the NICU, and public insurance status). The model also accounted for collinear variables, such as birth weight and IUGR. Additional perinatal factors (such as breast milk exposure, parent history of asthma, or maternal smoking during pregnancy) were ultimately not included due to unreliable documentation in clinical records or lack of available data, because nearly all neonates are referred to our NICU from prior institutions. A more limited multivariable model was then investigated more rigorously, including only variables that had higher clinical and statistical significance in the larger model (MRI score, GA, birth weight, multiparity, systemic PH medications, and pneumonia). The level for statistical significance was set at P less than 0.05 for all analyses.

Patients without BPD were excluded from univariate and multivariable models (*see* Discussion section).

Results

Typical images, level of respiratory support at discharge, and MRI scores across the spectrum of BPD severities are presented in Figure 1. Mean (±SE) MRI scores for

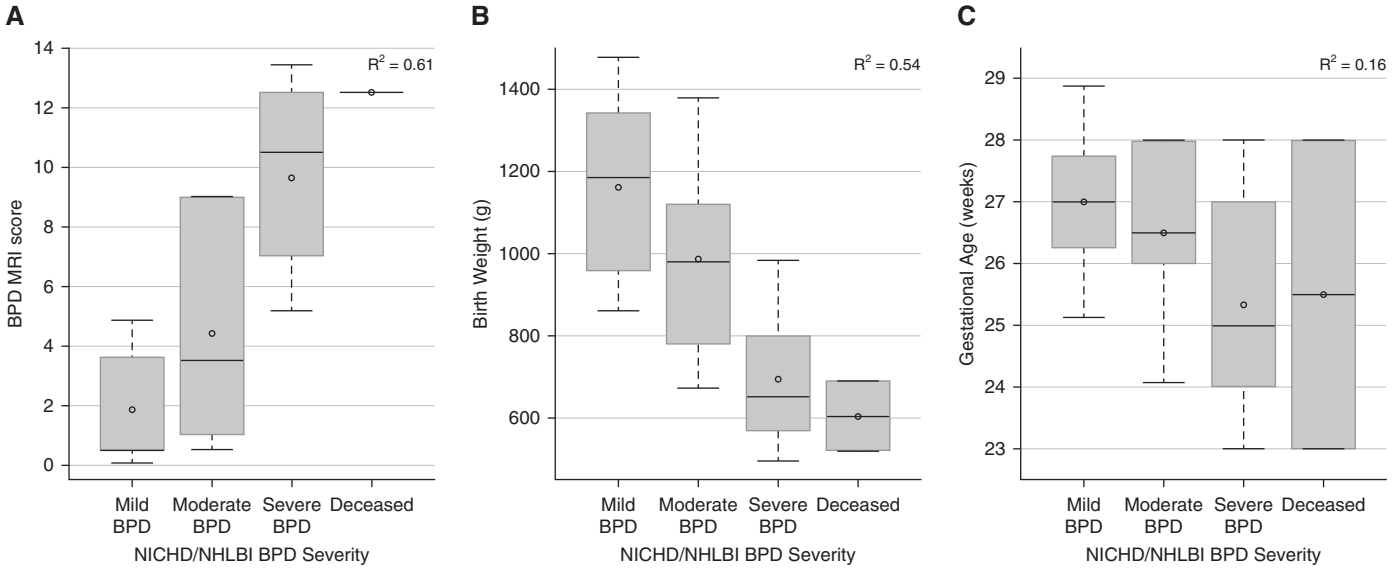

Figure 3. Correlations of National Institute of Child Health and Human Development (NICHD) bronchopulmonary dysplasia (BPD) severity (mild, moderate, severe, and deceased due to lung disease) to magnetic resonance imaging (MRI) score (*A*; $P < 0.0001$), birth weight (*B*; $P < 0.0001$), and gestational age (*C*; $P = 0.13$) (ANOVA). Plot elements are represented as follows: mean (circle); median (horizontal line); interquartile range (gray box); and 9–91% data (whiskers).

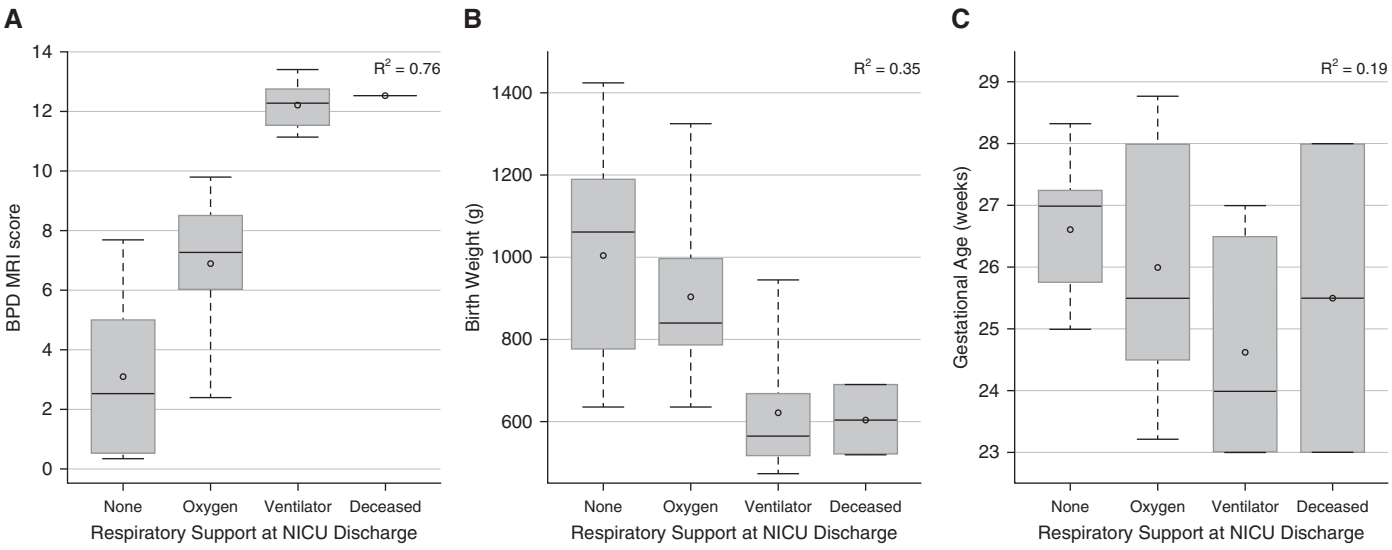

Figure 4. Correlations of respiratory support at neonatal ICU (NICU) discharge (room air, oxygen, ventilator, and deceased due to lung disease) to magnetic resonance imaging (MRI) score (*A*; $P < 0.0001$), birth weight (*B*; $P = 0.007$), and gestational age (*C*; $P = 0.12$) (ANOVA). Plot elements are represented as follows: mean (circle); median (horizontal line); interquartile range (gray box); and 9–91% data (whiskers). BPD = bronchopulmonary dysplasia.

patient groups were: term control, 0.5 (±0.4); preterm control, 0.9 (±0.8); mild BPD, 1.9 (±2.0); moderate BPD, 4.4 (±4.0); severe BPD, 9.6 (±3.0); and deceased from BPD, 12.5 (±0.0) (Figure 2). Interreader reliability for scores was good ($r = 0.86$, 95% confidence interval [CI] = 0.76–0.92).

NICHD BPD severity (Figure 3), respiratory support at NICU discharge (Figure 4), and respiratory support at 40-weeks PMA (Figure 5) correlated well with MRI score, fairly well with birth weight, and poorly with GA. The superiority of MRI scores was greater for concrete clinical outcomes (respiratory support at 40-wk PMA and NICU discharge) than for NICHD BPD severity. For this cohort, NICU discharge (or death) occurred approximately 4 weeks after MRI was performed (2, 4, and 5 wk for mild, moderate, and severe BPD, respectively). NICHD severity level was not necessarily indicative of NICU discharge support (*see* Table 3): subjects with moderate BPD were equally split between discharge on oxygen and discharge on room air, and three subjects with severe BPD were discharged on room air, whereas two subjects with severe BPD died from pulmonary morbidities.

In the stepwise selection regression models, duration of ventilator support was significantly predicted by MRI score ($R^2 = 0.78$), whereas birth weight and GA were not significant ($P > 0.2$); days on ventilator support increased by 12.9 (±1.3) (±SE) days per 1 point increase in MRI score. Duration of any PPV was significantly

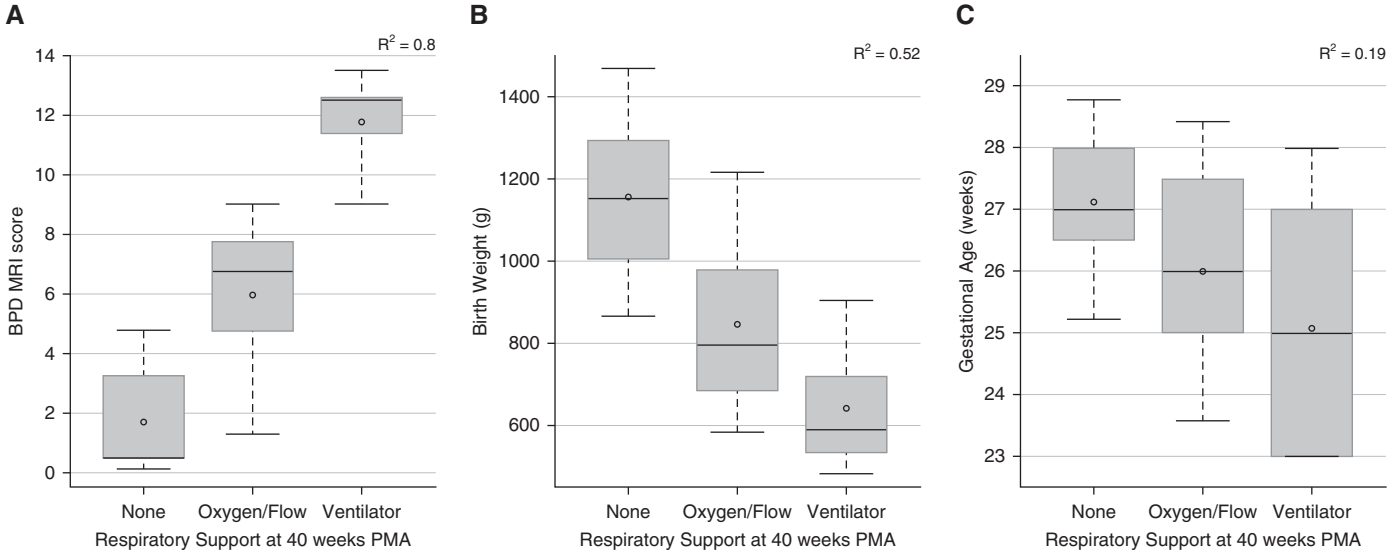

Figure 5. Correlations of respiratory support at 40-weeks postmenstrual age (PMA) (room air, oxygen/flow, and ventilator) to magnetic resonance imaging (MRI) score (*A*; $P < 0.0001$), birth weight (*B*; $P < 0.0001$), and gestational age (*C*; $P = 0.04$) (ANOVA). Plot elements are represented as follows: mean (circle); median (horizontal line); interquartile range (gray box); and 9–91% data (whiskers). BPD = bronchopulmonary dysplasia.

Table 3. Frequency Distribution of Bronchopulmonary Dysplasia Severity and Levels of Respiratory Support at Neonatal Intensive Care Unit Discharge

NICU Discharge Support	NICHD BPD Severity		
	Mild	Moderate	Severe
None	7	3	3
Oxygen	0	3	5
Ventilator	0	0	8
Deceased	0	0	2

Definition of abbreviations: BPD = bronchopulmonary dysplasia; NICHD = National Institute of Child Health and Human Development; NICU = neonatal ICU.
The results show that diagnosed severity is not necessarily indicative of respiratory outcomes at discharge.

predicted by MRI score and birth weight (partial $R^2 = 0.77$ and 0.07, respectively, with total $R^2 = 0.85$), whereas GA was not significant ($P > 0.2$); days on any PPV increased by 7.5 ($\pm$1.1) days per 1 point increase in MRI score. Similarly, duration of any support was significantly predicted by MRI score and birth weight (partial $R^2 = 0.59$ and 0.11, respectively, with total $R^2 = 0.71$), whereas GA was not significant ($P > 0.2$); days on any support increased by 4.3 ($\pm$1.3) days per 1 point increase in MRI score.

In the general linear models, sex, race, IUGR, postnatal growth failure, patent ductus arteriosus, atrial septal defect, diuretics, antenatal steroids, postnatal steroids, surfactant, highest level of respiratory support in the NICU, and insurance status had no impact on duration of any respiratory support levels. Accounting for GA, birth weight, multiparous pregnancy, need for systemic PH therapies, and occurrences of pneumonia in the NICU, MRI score significantly predicted days on ventilator support (8.1 [95% CI = 3.6–12.6] more days per 1 point increase in MRI score; total $R^2 = 0.86$), days on any PPV (6.7 [95% CI = 4.3–9.6] more days per 1 point increase in MRI score; total $R^2 = 0.91$), and days on any support (6.3 [95% CI = 2.8–9.7] more days per 1 point increase in MRI score; total $R^2 = 0.77$). In this multivariable prediction model, MRI score was always the strongest predictor of duration of all respiratory support levels (Table 4).

Eight subjects with BPD were on PH therapy at discharge from the NICU (or time of death). According to clinical records, all eight subjects were on ventilator support or died as the primary outcome, with clinically assessed lung disease independent of PH that necessitated mechanical ventilation. Three subjects with BPD were treated with PH therapy that was discontinued before NICU discharge or death; in each of these cases, use of respiratory support continued past the time point at which PH therapy was discontinued, such that PH was not the primary factor in duration of respiratory support.

Five subjects with BPD had documentation of apnea of prematurity contributing to prolonged oxygen use; four of these subjects were off respiratory support before or by 40-weeks PMA, whereas one subject continued to use supplemental oxygen until 48-weeks PMA, with available clinical data not indicative of whether oxygen dependency was due to apnea of prematurity or additional nonapneic hypoxemia.

Table 4. A General Linear Model Predicting Duration of Various Levels of Respiratory Support, Censored to 150 Days of Life

Support Level Duration Predicted (Censored to 150 d of Life)	Total R^2 of Model	*P* Value of Significant Variables*	Increase in Days of Support Duration per 1 Point Increase in MRI Score (95% CI)
Any support	0.77	MRI score: 0.001 Birth weight: 0.002	6.3 (2.8–9.7)
Any PPV	0.91	MRI score: <0.0001 Birth weight: 0.002	6.7 (4.3–9.6)
Ventilator	0.86	MRI score: 0.001 PH therapy: 0.025	8.1 (3.6–12.6)

Definition of abbreviations: CI = confidence interval; MRI = magnetic resonance imaging; PH = pulmonary hypertension; PPV = positive pressure ventilation.
Predictor variables included MRI score, gestational age, birth weight, multiparity, systemic PH medications, and pneumonia during neonatal ICU admission. MRI score was always the most significant predictor.
*All other predictor variables were not significant in the model ($P > 0.05$).

Discussion

Quiet-breathing neonatal pulmonary MRI can assess structural abnormalities of BPD without requiring sedation or ionizing radiation. This work represents the first results demonstrating that pulmonary MRI in neonatal patients with BPD can independently describe disease severity and predict short-term clinical outcomes better than individual standard clinical measures. Although both birth weight and MRI score correlate similarly with NICHD severity, NICHD severity level is not predictive of eventual discharge support; the heterogeneous relationship between clinical BPD severity level and short-term respiratory outcomes (Table 3), particularly in infants with moderate and severe BPD, signifies the somewhat insufficient current definition of clinical BPD severity. The results of the present study indicate that MRI findings are more informative than BPD severity grading based on the traditional NICHD definition. Furthermore, this work suggests that MRI can play an important, possibly even critical, role in revising the definition of BPD, particularly if implemented at even earlier time points, and may aid in applying precision medicine techniques for individualized disease trajectories.

CT scoring systems of infant BPD already exist (35, 36), but concerns over ionizing radiation exposure and sedation requirements for a pediatric CT scan (15–19) make the nonionizing, nonsedated MRI techniques used in this study a safer choice, particularly for longitudinal imaging of neonatal subjects. The MRI scoring system used here could be refined to include only categories of greatest significance, modify terminology to be more widely understandable, and reduce scoring subjectivity. The addition of quantitative assessments of the structural patterns and distribution of parenchymal disease to ordinal scoring schemes is desirable, and complements radiological phenotyping of disease. Previous work on

CT of cystic fibrosis and interstitial lung diseases has achieved quantitative measures and textural analysis (37–39), which decrease variation in inter- and intrareader scoring and reduces evaluation time, but such work has yet to be extended to MR images or to the evaluation of neonatal BPD.

This study was performed using a unique, small-footprint, neonatal-sized MRI scanner sited within our NICU. However, implementation of this technique does not require a dedicated NICU system; these scans are translatable to any adult-sized scanner with appropriately sized coils for neonatal chest imaging. Furthermore, GRE sequences are readily available on any conventional scanner, and all three major MRI manufacturers have sequences in development similar to the UTE sequence implemented here.

Historically, pulmonary MRI has been challenging due to the rapid proton signal decay ($T_2^* \approx 2$ ms for nonfibrotic lung parenchyma at 1.5 T). For TE values approximately equal to or longer than the parenchymal T_2^*, MR signal from nonfibrotic tissue is not adequately acquired, and thus is visualized as a low-intensity region in the MR image. Thus, short TE values, like those implemented for the UTE sequence, are essential for a complete evaluation of normal tissue and hypodense tissue (alveolar simplification, emphysema, cysts, etc.; Table 2). Furthermore, MR images can provide normalized signal intensities nearly identical to CT densities through selection of MR parameters that yield a near-proton-density regime (i.e., small FA, $TE \leqslant T_2^*$) (27). However, a sequence with a TE near parenchymal T_2^*, as implemented with the GRE sequence here, can complement the proton-density UTE images by yielding a higher contrast between lung parenchyma and soft tissues (fibrotic, interstitial, vasculature, etc.; Table 2).

Typically, pediatric lung function is assessed clinically with pulmonary function tests (PFTs) (40–42). However, PFT methods are effort dependent and can be unreliable, particularly in children. In contrast, quantitative, imaging-based metrics are more reliable, and have the potential to be more effective in precisely evaluating disease severity. Indeed, the use of hyperpolarized (HP) ^{3}He and ^{129}Xe gas MRI in both adult and pediatric lung diseases has high sensitivity via ventilation (43–45), restricted diffusion (46–49), and dissolved-phase techniques (50–55). Importantly, these techniques provide regional information about respiratory structure and function, which PFT techniques cannot, and can be combined with structural images from ^{1}H MRI, such as those used in the present study. The application of HP gas MRI methods to infants and preschool-aged children has thus far been limited (46, 48, 56), but, with established safety records in adults (57) and pediatrics (58), there is strong potential for HP gas MRI techniques to further characterize structural and functional pulmonary pathologies in very young infants with BPD.

There is great interest in assessing the relationship between early-life biomarkers, such as those provided by MRI, and longer-term outcomes, such as preschool- and school-aged respiratory symptoms, intolerance for exercise, rehospitalizations, and cognitive testing (59). A limitation of the current study is that the majority of the cohort is still in infancy. Even so, the short-term results here censored to 150 days of life effectively capture which patients are likely to wean from respiratory support in the NICU compared with those likely heading toward longer-term support. In future studies, we hope to demonstrate that phenotyping of disease through earlier MRI will yield an ability to personalize early clinical care by assessing likelihood of responsiveness to individual treatments (such as steroids), which will likely improve long-term outcomes. Furthermore, longitudinal studies can shed light on the time course of parenchymal abnormalities during standard clinical treatments in the neonatal period and beyond.

Another limitation of our study is the uneven distribution of clinical severity, potentially reflecting referral bias; as a primarily referral-based NICU with few in-born neonates, only preterm infants with severe sequelae of prematurity or infants with other complex comorbidities are typically admitted. The uneven distribution of severity and relatively modest sample size necessarily led to small sample sizes in subgroups (e.g., subjects with mild or moderate BPD, or in those with IUGR). The referral patterns also led to incomplete representation of GAs; there were no subjects with GAs of 30–33 weeks.

In conclusion, early-life pulmonary MRI can independently quantify the structural abnormalities of neonatal BPD and predict short-term outcomes better than any individual standard clinical measure, without requiring sedation or ionizing radiation. These results demonstrate an ability to select preterm neonatal patients at increased risk for respiratory morbidities, and therefore support the wider implementation of imaging at even earlier time points as a predictor of disease trajectories. Importantly, the regional and structural information inherent in tomographic imaging provides the potential to image phenotype disease and better describe severity, which may be used to personalize treatment and monitor the efficacy of new therapies. Because pulmonary MRI can be used safely for serial assessment, this technique has the potential to define the trajectory of neonatal pulmonary disease associated with extreme prematurity. ■

Author disclosures are available with the text of this article at www.atsjournals.org.

Acknowledgment: The authors thank the patients and families who participated in the study.

References

1. Stoll BJ, Hansen NI, Bell EF, Shankaran S, Laptook AR, Walsh MC, *et al.*; Eunice Kennedy Shriver National Institute of Child Health and Human Development Neonatal Research Network. Neonatal outcomes of extremely preterm infants from the NICHD Neonatal Research Network. *Pediatrics* 2010;126:443–456.
2. Bhandari A, McGrath-Morrow S. Long-term pulmonary outcomes of patients with bronchopulmonary dysplasia. *Semin Perinatol* 2013;37: 132–137.
3. Gibson AM, Doyle LW. Respiratory outcomes for the tiniest or most immature infants. *Semin Fetal Neonatal Med* 2014;19:105–111.
4. Simpson SJ, Hall GL, Wilson AC. Lung function following very preterm birth in the era of 'new' bronchopulmonary dysplasia. *Respirology* 2015;20:535–540.
5. Northway WH Jr, Rosan RC, Porter DY. Pulmonary disease following respirator therapy of hyaline-membrane disease: bronchopulmonary dysplasia. *N Engl J Med* 1967;276:357–368.
6. Jobe AH, Bancalari E. Bronchopulmonary dysplasia. *Am J Respir Crit Care Med* 2001;163:1723–1729.

7. Johnson TJ, Patel AL, Jegier BJ, Engstrom JL, Meier PP. Cost of morbidities in very low birth weight infants. *J Pediatr* 2013;162: 243–249.e1.
8. Poindexter BB, Feng R, Schmidt B, Aschner JL, Ballard RA, Hamvas A, *et al*.; Prematurity and Respiratory Outcomes Program. Comparisons and limitations of current definitions of bronchopulmonary dysplasia for the Prematurity and Respiratory Outcomes Program. *Ann Am Thorac Soc* 2015;12:1822–1830.
9. Morrow LA, Wagner BD, Ingram DA, Poindexter BB, Schibler K, Cotten CM, *et al*. Antenatal determinants of bronchopulmonary dysplasia and late respiratory disease in preterm infants. *Am J Respir Crit Care Med* 2017;196:364–374.
10. Shepherd EG, Nelin LD. Preterm birth, bronchopulmonary dysplasia, and long-term respiratory disease. *Am J Respir Crit Care Med* 2017; 196:264–265.
11. Babata K, McGuirl J. Are we ready to modify our definition of bronchopulmonary dysplasia (BPD) to improve prognostication? *J Perinatol* 2018;38:203–205.
12. D'Alessandro A, Nozik-Grayck E, Stenmark KR. Identification of infants at risk for chronic lung disease at birth: potential for a personalized approach to disease prevention. *Am J Respir Crit Care Med* 2017; 196:951–952.
13. Abman SH, Ivy DD, Archer SL, Wilson K; AHA/ATS Joint Guidelines for Pediatric Pulmonary Hypertension Committee. Executive summary of the American Heart Association and American Thoracic Society joint guidelines for pediatric pulmonary hypertension. *Am J Respir Crit Care Med* 2016;194:898–906.
14. Ivy DD, Abman SH, Barst RJ, Berger RM, Bonnet D, Fleming TR, *et al*. Pediatric pulmonary hypertension. *J Am Coll Cardiol* 2013; 62(25 Suppl):D117–D126.
15. Miglioretti DL, Johnson E, Williams A, Greenlee RT, Weinmann S, Solberg LI, *et al*. The use of computed tomography in pediatrics and the associated radiation exposure and estimated cancer risk. *JAMA Pediatr* 2013;167:700–707.
16. Brenner D, Elliston C, Hall E, Berdon W. Estimated risks of radiation-induced fatal cancer from pediatric CT. *AJR Am J Roentgenol* 2001; 176:289–296.
17. Pearce MS, Salotti JA, Little MP, McHugh K, Lee C, Kim KP, *et al*. Radiation exposure from CT scans in childhood and subsequent risk of leukaemia and brain tumours: a retrospective cohort study. *Lancet* 2012;380:499–505.
18. Cravero JP, Beach ML, Blike GT, Gallagher SM, Hertzog JH; Pediatric Sedation Research Consortium. The incidence and nature of adverse events during pediatric sedation/anesthesia with propofol for procedures outside the operating room: a report from the Pediatric Sedation Research Consortium. *Anesth Analg* 2009;108:795–804.
19. Mahmoud M, Towe C, Fleck RJ. CT chest under general anesthesia: pulmonary, anesthetic and radiologic dilemmas. *Pediatr Radiol* 2015; 45:977–981.
20. Walkup LL, Woods JC. Newer imaging techniques for bronchopulmonary dysplasia. *Clin Perinatol* 2015;42:871–887.
21. Walkup LL, Tkach JA, Higano NS, Thomen RP, Fain SB, Merhar SL, *et al*. Quantitative magnetic resonance imaging of bronchopulmonary dysplasia in the neonatal intensive care unit environment. *Am J Respir Crit Care Med* 2015;192:1215–1222.
22. Yu J, Xue Y, Song HK. Comparison of lung T2* during free-breathing at 1.5 T and 3.0 T with ultrashort echo time imaging. *Magn Reson Med* 2011;66:248–254.
23. Johnson KM, Fain SB, Schiebler ML, Nagle S. Optimized 3D ultrashort echo time pulmonary MRI. *Magn Reson Med* 2013;70:1241–1250.
24. Hahn AD, Higano NS, Walkup LL, Thomen RP, Cao X, Merhar SL, *et al*. Pulmonary MRI of neonates in the intensive care unit using 3D ultrashort echo time and a small footprint MRI system. *J Magn Reson Imaging* 2017;45:463–471.
25. Higano NS, Hahn AD, Tkach JA, Cao X, Walkup LL, Thomen RP, *et al*. Retrospective respiratory self-gating and removal of bulk motion in pulmonary UTE MRI of neonates and adults. *Magn Reson Med* 2017; 77:1284–1295.
26. Hatabu H, Alsop DC, Listerud J, Bonnet M, Gefter WB. T2* and proton density measurement of normal human lung parenchyma using submillisecond echo time gradient echo magnetic resonance imaging. *Eur J Radiol* 1999;29:245–252.
27. Higano NS, Fleck RJ, Spielberg DR, Walkup LL, Hahn AD, Thomen RP, *et al*. Quantification of neonatal lung parenchymal density via ultrashort echo time MRI with comparison to CT. *J Magn Reson Imaging* 2017;46:992–1000.
28. Higano NS, Fleck RJ, Spielberg DR, Walkup LL, Hahn AD, Thomen RP, *et al*. MRI-based scoring of bronchopulmonary dysplasia (BPD) correlates with disease severity and short-term outcomes [abstract]. *Am J Respir Crit Care Med* 2017;195:A7200.
29. Higano NS, Fleck RJ, Spielberg DR, Walkup LL, Hahn AD, Tkach JA, *et al*. Quantitative characterization of bronchopulmonary dysplasia severity using neonatal pulmonary MRI and correlation to short-term outcomes [abstract]. Presented at the Annual Meeting of the Radiological Society of North America. November 28, 2017, Chicago, IL. Abstract 17005078.
30. Higano NS, Spielberg DR, Fleck RJ, Schapiro AH, Walkup LL, Hahn AD, *et al*. Neonatal pulmonary MRI of bronchopulmonary dysplasia predicts short-term clinical outcomes [abstract]. *Am J Respir Crit Care Med* 2018;197:A7384.
31. Tkach JA, Hillman NH, Jobe AH, Loew W, Pratt RG, Daniels BR, *et al*. An MRI system for imaging neonates in the NICU: initial feasibility study. *Pediatr Radiol* 2012;42:1347–1356.
32. Tkach JA, Merhar SL, Kline-Fath BM, Pratt RG, Loew WM, Daniels BR, *et al*. MRI in the neonatal ICU: initial experience using a small-footprint 1.5-T system. *AJR Am J Roentgenol* 2014;202:W95–W105.
33. Tkach JA, Li Y, Pratt RG, Baroch KA, Loew W, Daniels BR, *et al*. Characterization of acoustic noise in a neonatal intensive care unit MRI system. *Pediatr Radiol* 2014;44:1011–1019.
34. Merhar SL, Tkach JA, Woods JC, South AP, Wiland EL, Rattan MS, *et al*. Neonatal imaging using an on-site small footprint MR scanner. *Pediatr Radiol* 2017;47:1001–1011.
35. Ochiai M, Hikino S, Yabuuchi H, Nakayama H, Sato K, Ohga S, *et al*. A new scoring system for computed tomography of the chest for assessing the clinical status of bronchopulmonary dysplasia. *J Pediatr* 2008;152:90–95, 95.e1–3.
36. van Mastrigt E, Logie K, Ciet P, Reiss IK, Duijts L, Pijnenburg MW, *et al*. Lung CT imaging in patients with bronchopulmonary dysplasia: a systematic review. *Pediatr Pulmonol* 2016;51:975–986.
37. Rosenow T, Oudraad MC, Murray CP, Turkovic L, Kuo W, de Bruijne M, *et al*.; Australian Respiratory Early Surveillance Team for Cystic Fibrosis (AREST CF). PRAGMA-CF: a quantitative structural lung disease computed tomography outcome in young children with cystic fibrosis. *Am J Respir Crit Care Med* 2015;191:1158–1165.
38. Hoffman EA, Reinhardt JM, Sonka M, Simon BA, Guo J, Saba O, *et al*. Characterization of the interstitial lung diseases via density-based and texture-based analysis of computed tomography images of lung structure and function. *Acad Radiol* 2003;10: 1104–1118.
39. Jacob J, Bartholmai BJ, Brun AL, Egashira R, Rajagopalan S, Karwoski R, *et al*. Evaluation of visual and computer-based CT analysis for the identification of functional patterns of obstruction and restriction in hypersensitivity pneumonitis. *Respirology* 2017;22: 1585–1591.
40. Lo J, Zivanovic S, Lunt A, Alcazar-Paris M, Andradi G, Thomas M, *et al*. Longitudinal assessment of lung function in extremely prematurely born children. *Pediatr Pulmonol* 2018;53:324–331.
41. Thunqvist P, Tufvesson E, Bjermer L, Winberg A, Fellman V, Domellöf M, *et al*. Lung function after extremely preterm birth—a population-based cohort study (EXPRESS). *Pediatr Pulmonol* 2018;53:64–72.
42. Um-Bergström P, Hallberg J, Thunqvist P, Berggren-Broström E, Anderson M, Adenfelt G, *et al*. Lung function development after preterm birth in relation to severity of bronchopulmonary dysplasia. *BMC Pulm Med* 2017;17:97.
43. Koumellis P, van Beek EJ, Woodhouse N, Fichele S, Swift AJ, Paley MN, *et al*. Quantitative analysis of regional airways obstruction using dynamic hyperpolarized ^{3}He MRI—preliminary results in children with cystic fibrosis. *J Magn Reson Imaging* 2005;22: 420–426.
44. Thomen RP, Walkup LL, Roach DJ, Cleveland ZI, Clancy JP, Woods JC. Hyperpolarized ^{129}Xe for investigation of mild cystic fibrosis lung disease in pediatric patients. *J Cyst Fibros* 2017;16: 275–282.

45. Kanhere N, Couch MJ, Kowalik K, Zanette B, Rayment JH, Manson D, *et al*. Correlation of lung clearance index with hyperpolarized ^{129}Xe magnetic resonance imaging in pediatric subjects with cystic fibrosis. *Am J Respir Crit Care Med* 2017;196:1073–1075.
46. Cadman RV, Lemanske RF Jr, Evans MD, Jackson DJ, Gern JE, Sorkness RL, *et al*. Pulmonary ^{3}He magnetic resonance imaging of childhood asthma. *J Allergy Clin Immunol* 2013;131:369–376.e1–5.
47. Fishman EF, Quirk JD, Sweet SC, Woods JC, Gierada DS, Conradi MS, *et al*. What makes a good pediatric transplant lung: insights from in vivo lung morphometry with hyperpolarized ^{3} He magnetic resonance imaging. *Pediatr Transplant* 2017;21:e12886.
48. Altes TA, Meyer CH, Mata JF, Froh DK, Paget-Brown A, Gerald Teague W, *et al*. Hyperpolarized helium-3 magnetic resonance lung imaging of non-sedated infants and young children: a proof-of-concept study. *Clin Imaging* 2017;45:105–110.
49. Higano NS, Thomen R, Parks K, Huyck H, Hahn A, Fain SB, *et al*. Hyperpolarized ^{3}He gas MRI in infant lungs: investigating airspace size [abstract]. *Am J Respir Crit Care Med* 2017;195:A2663.
50. Ruppert K, Mata JF, Brookeman JR, Hagspiel KD, Mugler JP III. Exploring lung function with hyperpolarized (129)Xe nuclear magnetic resonance. *Magn Reson Med* 2004;51:676–687.
51. Wang Z, Robertson SH, Wang J, He M, Virgincar RS, Schrank GM, *et al*. Quantitative analysis of hyperpolarized ^{129} Xe gas transfer MRI. *Med Phys* 2017;44:2415–2428.
52. Mugler JP III, Altes TA. Hyperpolarized ^{129}Xe MRI of the human lung. *J Magn Reson Imaging* 2013;37:313–331.
53. Wang JM, Robertson SH, Wang Z, He M, Virgincar RS, Schrank GM, *et al*. Using hyperpolarized ^{129}Xe MRI to quantify regional gas transfer in idiopathic pulmonary fibrosis. *Thorax* 2018;73:21–28.
54. Stewart NJ, Leung G, Norquay G, Marshall H, Parra-Robles J, Murphy PS, *et al*. Experimental validation of the hyperpolarized ^{129} Xe chemical shift saturation recovery technique in healthy volunteers and subjects with interstitial lung disease. *Magn Reson Med* 2014; 74:196–207.
55. Ebner L, Kammerman J, Driehuys B, Schiebler ML, Cadman RV, Fain SB. The role of hyperpolarized ^{129}xenon in MR imaging of pulmonary function. *Eur J Radiol* 2017;86:343–352.
56. Flors L, Mugler JP III, Paget-Brown A, Froh DK, de Lange EE, Patrie JT, *et al*. Hyperpolarized helium-3 diffusion-weighted magnetic resonance imaging detects abnormalities of lung structure in children with bronchopulmonary dysplasia. *J Thorac Imaging* 2017;32:323–332.
57. Shukla Y, Wheatley A, Kirby M, Svenningsen S, Farag A, Santyr GE, *et al*. Hyperpolarized ^{129}Xe magnetic resonance imaging: tolerability in healthy volunteers and subjects with pulmonary disease. *Acad Radiol* 2012;19:941–951.
58. Walkup LL, Thomen RP, Akinyi TG, Watters E, Ruppert K, Clancy JP, *et al*. Feasibility, tolerability and safety of pediatric hyperpolarized ^{129}Xe magnetic resonance imaging in healthy volunteers and children with cystic fibrosis. *Pediatr Radiol* 2016;46:1651–1662.
59. Brumbaugh JE, Colaizy TT, Patel NM, Klein JM. The changing relationship between bronchopulmonary dysplasia and cognition in very preterm infants. *Acta Paediatr* 2018;107:1339–1344.